Jinst

PUBLISHED BY IOP PUBLISHING FOR SISSA

RECEIVED: *December 4, 2010*
REVISED: *February 15, 2011*
ACCEPTED: *February 21, 2011*
PUBLISHED: *March 10, 2011*

High resolution optical calorimetry for synchrotron microbeam radiation therapy

T. Ackerly,[a] J.C. Crosbie,[a,b,1] A. Fouras,[c] G.J.Sheard,[d] S. Higgins[c] and R.A. Lewis[e]

[a] *William Buckland Radiotherapy Centre, The Alfred Hospital, Commercial Road, Melbourne, Australia*
[b] *Department of Obstetrics & Gynaecology, University of Melbourne, Flemington Road and Grattan Street, Melbourne, Australia*
[c] *Division of Biological Engineering, Monash University, Wellington Road, Melbourne, Australia*
[d] *Department of Mechanical and Aerospace Engineering, Monash University, Wellington Road, Melbourne, Australia*
[e] *Monash Centre for Synchrotron Science, Monash University, Wellington Road, Melbourne, Australia*

E-mail: jcrosbie@unimelb.edu.au

ABSTRACT: We propose the application of optical calorimetry to measure the peak to valley ratio for synchrotron microbeam radiation therapy (MRT). We use a modified Schlieren approach known as reference image topography (RIT) which enables one to obtain a map of the rate of change of the refractive index in a water bath from which the absorbed dose can be determined with sufficient spatial accuracy to determine the peak to valley ratio. We modelled the calorimetric properties of X-rays using a heated wire in a water bath. Our RIT system comprised a light source, a textured reference object and a camera and lens combination. We measured temperature contours and showed a plume rising from the heated wire. The total temperature change in water was 12 degrees C, 500 times greater than the calculated change from a 1 ms exposure on a synchrotron. At 1.0 ms, thermal diffusion will be the major cause of uncertainty in determining the peak to valley ratio, and we calculate thermal diffusion will reduce the measured peak to valley ratio to 76% of its initial value, but the individual microbeams will still resolve. We demonstrate proof of concept for measuring X-ray dose using a modified RIT method.

KEYWORDS: Dosimetry concepts and apparatus; Microdosimetry and nanodosimetry; Radiotherapy concepts

[1] Corresponding author.

© 2011 IOP Publishing Ltd and SISSA

doi:10.1088/1748-0221/6/03/P03003

2011 JINST 6 P03003

Contents

1 Introduction **1**
- 1.1 Synchrotron microbeam radiation therapy (MRT) 1
- 1.2 Holographic interferometry (HI) 2
- 1.3 Reference image topography (RIT) 3

2 Methods **4**

3 Results **6**

4 Discussion **6**

2011 JINST 6 P03003

1 Introduction

We propose the application of optical calorimetry to solve the problem of measuring the peak to valley dose ratio for synchrotron microbeam radiation therapy (MRT). MRT represents a paradigm shift in radiotherapy thinking and has shown great promise in pre-clinical studies on tumour-inoculated rodents [1–4]. A major factor hampering progress towards clinical acceptance of MRT is the lack of a suitable method to measure the absorbed dose distribution from a lattice of microbeams owing to very steep dose gradients [5]. We propose a calorimetric method derived from earlier work on holographic interferometry that utilizes changes in the refractive index of water to measure temperature changes that directly relate to the absolute absorbed dose [6–8].

1.1 Synchrotron microbeam radiation therapy (MRT)

MRT is an experimental radiotherapy technique that involves fractionating the dose in space rather than in time [9]. MRT uses diagnostic energy X-rays (50–250 keV) rather than the megavoltage beams produced by hospital linear accelerators. MRT has shown great efficacy in tumour-bearing rodent models with remarkable sparing of normal tissue and is under consideration for clinical use in Europe [10]. The imaging and medical beamline at the Australian Synchrotron has been designed to enable this technique in which the high flux, X-ray beam from the synchrotron is segmented into an array, or lattice, of narrow micro-planar beams, typically 25 μm wide and separated by 200 μm. Our MRT research group has been conducting radiobiological and physical studies of MRT using the SPring-8 synchrotron in Japan and the Australian Synchrotron. In one experiment, we showed significant survival ($p < 0.0005$) for tumour-inoculated mice treated with MRT compared to un-irradiated controls [1].

MRT has several peculiar and beguiling properties, which challenge many of the current paradigms in conventional radiation therapy; (i) Normal tissue appears exceptionally resistant to hundreds of Gray of peak, in-beam MRT doses [11, 12], (ii) Malignant tissue appears to respond to MRT by significant growth delay and, in some cases, complete tumour ablation, despite the

small fraction of the tumour mass irradiated with the high dose microbeams [2, 3, 13–16], (iii) The ratio between the dose in the peaks of the microbeams and the dose in the valleys between the microbeams has strong biological significance [12–14, 17]. Given that cells in the MRT beamlets receive radiation doses well in excess of lethal radiation dose, it is reasonable to assume that tissue survival correlates to a large degree with the valley dose. Primary variables influencing valley dose are mean X-ray energy, beamlet width, beamlet spacing, and radiation dose in the peaks.

The geometrical configuration of the microbeams is a crucial factor in the success of MRT but the dose gradients of hundreds of Gray over tens of micron present a significant challenge for dosimetry. Since the microbeams are 25 microns wide and are separated by 200 microns, measuring the peak to valley ratio requires spatial resolution beyond the capabilities of conventional ionisation chamber-based dosimetry. Consequently, the majority of publications pertaining to MRT dosimetry employ Monte Carlo computer simulations to model the radiation transport and dose deposition in water [18–21]. Some research groups have published experimental data using Metal Oxide Semiconducting Field Effect Transistors (MOSFET) as an X-ray microbeam dosimeter [22–24] and have compared them with Monte Carlo simulation results [19, 20, 25] and reported acceptable agreement on a micron scale. Other research groups also reported on their experiences with thermo-luminescent dosimeters (TLD) with mixed success [26]. Our own group reported the use of radiochromic films of different sensitivity to measure the peak and valley doses separately [5]. Using film and microdensitometry is a useful way to experimentally quantify MRT dosimetry; however a downside to the two-film dosimetry technique is the large uncertainty (±25%) associated with it [5].

A number of critical questions remain unanswered; (1) what is the optimum in-beam dose for MRT? (2) What is the optimum peak-to-valley dose ratio for successful MRT (maximal tumour control and minimal normal tissue toxicity)? (3) Does the optimum ratio vary with the tissue and cell types being irradiated? (4) What is the optimum energy spectrum for MRT? (5) What are the threshold doses for damage and death for various cell types as a function of the beam geometries? (6) What are the optimal dose rates? Clearly investigations into alternative dosimetry methods for MRT are worthwhile,

1.2 Holographic interferometry (HI)

The idea to use optical calorimetry for radiation dosimetry originates from early experiments with holographic interferometry for dosimetry in the 1970's [6–8, 27]. The HI method is based upon the knowledge that practically all imparted radiation on an absorbing medium is converted to heat [6]. A calorimetric technique may then be used to infer the beam energy distribution based upon the temperature rise of the absorbing medium after irradiation [28], as described mathematically in equation (1.1).

$$D = \frac{c_p \lambda}{x\left(\frac{dn}{dT}\right)} \tag{1.1}$$

Where D is the absorbed dose per interference fringe in J/kg, C_p is the specific heat capacity (J/kgK) of the irradiated medium (e.g. liquid water), λ is the wavelength of the illuminating light source (m), x is the path length of the irradiation cell (m) and dn/dT is the temperature coefficient of the refractive index of the irradiated medium (K^{-1}). The specific heat capacity and the temperature coefficient of liquid water are well characterized. By placing a transparent medium (such as a

2011 JINST 6 P03003

container of water) in the path of the beam, the temperature rise and spatial temperature distribution that builds up within it immediately after irradiation can be directly related to the dose absorbed by the subject. Since the refractive index of the transparent medium is a function of temperature, local changes in refractive index are representative of the dose distribution.

The change in refractive index is approximately proportional to the change in temperature according to; $\Delta n = \Delta T \cdot dn/dT$, where dn/dT is the temperature coefficient of the refractive index. Tilton & Taylor [29] measured the refractive index as a function of temperature and Miller and McLaughlin [30] quoted Tilton & Taylor's work stating;

$$\frac{dn}{dT} = 0.93 \times 10^{-4} \text{ per degree C at } 21^{\circ}\text{C}$$

Further, within a temperature difference of 20°C to 30°C, dn/dT could be approximated as;

$$\frac{dn}{dT} \approx (300 + 30T) \times 10^{-7} \text{ per degree C}$$

More recently, Abbate et al. [31] provided data which showed the change in gradient of the refractive index with temperature (dn/dT) is on the order of 10^{-4} (0.01%) and can be considered linear over the range 0 to 30°C.

It is important to note the temperature distribution representing the absorbed dose distribution will remain for only a very short period (of the order of a few milliseconds) before thermal dissipation effects re-homogenise the temperature field. It is therefore necessary for both the irradiation time and the measurement time to be shorter than the thermal relaxation time. An interferometer is used to measure the refractive index changes. A beam splitter divides the laser wavefront into a reference and an object beam. The object beam traverses the irradiation cell twice and then combines with the reference beam, thus generating a hologram. Reconstruction of the hologram yields an interference pattern generated by the wavefronts passing through the cell before and after irradiation. These fringes correspond to the isodose distribution shown in figure 3 in [8]. In their publications, Miller, Hussmann and McLaughlin demonstrated a dose resolution of 3.5 Gy, for a 42 mm path length, and the spatial resolution capability of the holographic technique has been demonstrated by Charriere et al. [32] and Sheng et al. [33] to be about 1 micrometer using a holographic microscopic approach. The dose and spatial resolution may be improved by employing a multiple pass geometry to increase the path length x, or decrease the wavelength λ of the laser and hence improve the dose resolution, as suggested by Miller and McLaughlin [8].

1.3 Reference image topography (RIT)

The RIT idea is a further development of the early experiments with holographic interfereometry, described above, that is made possible by modern instrumentation. The method is capable of determining the dose in water and does not require a detector that would perturb the dose distribution. The calorimetric nature of the modified RIT method means that it is a so called "primary" technique, i.e. the absolute dose can be measured directly, without recourse to or cross calibration against another dosimeter such as an ionisation chamber.

The qualititave measurement of the temperature/refractive index of gases has been conducted using Schlieren imaging for well over three centuries [34]. A much newer, quantitative approach

2011 JINST 6 P03003

known as background-oriented Schlieren combines the concept of Schlieren with particle image velocimetry (PIV). A similar concept, known as reference image topography [35, 36], uses the accurate measurement of the apparent motion of a reference object to perform accurate, time-resolved measurements of the topography of a free liquid surface. A speckle pattern is projected through a water bath (the calorimeter) and the apparent motion of the speckle pattern before, during, and immediately after the irradiation is measured through a discretised cross-correlation approach (such as occurs in particle image velocimtery processing [37, 38]). The degree of apparent motion is directly related to the spatial rate of change of the refractive index and magnifcation of the system. The magnification is effectively given by the lens magnification and the optical path length between the changing medium and the reference object. For a known magnifcation, the method provides a measure of the spatial rate of change of the refractive index.

This spatial gradient of the refractive index can be integrated to give the refractive index and hence, in theory, the absorbed dose. To our knowledge, the RIT technique (or any similar method) has never been used previously to determine the absorbed dose from an X-ray beam. Within the physical constraints of the Australian Synchrotron medical beam line hutch enclosure (which limits the optical path length), the magnification factor can make the spatial resolution as small as 1 micron. The exposure time of the synchrotron can be set as low as 1.0 msec and the measurement time as low as 1 microsecond, constrained by the X-ray dose rate of the Synchrotron and the brightness of the light source respectively.

We can obtain preliminary RIT data more readily than HI data because the RIT equipment required is already available and operational. Sections 2 and 3 of this article describe our methodology and preliminary results respectively for acquiring modified RIT data from a heated wire in a water bath used as a model of an X-ray beam passing through a calorimeter.

2 Methods

Prior to testing with X-rays we have chosen to demonstrate the RIT system using a fine wire which provides a localised heat source to a bath of water. Figure 1 illustrates our heated wire model and the modified RIT imaging configuration. The method is simple and inexpensive to set up. The only components required are a simple illumination source, patterned reference object, and camera and lens combination. Importantly, there is no special requirement for accurate alignment of components.

The detector used in this system is a 2024×2024 pixel cooled CCD array (PCO.2000, PCO Germany), with a pixel size of 7.5 μm, and 1:1 macro lens (105 mm micro-Nikkor, Nikon, Japan). This was used with a frame rate of 15 frames per second and 100 μsec exposures. Due to the in-line configuration of the system, the optical efficiency is extremely high, allowing for such short exposures while utilising an inexpensive light source (a simple halogen light bulb). However, exposure times can be shortened further by the use of a more brilliant light source.

The camera is focused on the speckle pattern positioned on the front of the lamp and the water bath with wire is placed in between the light and the camera. The water is first left to settle, and a set of reference images are acquired. As the power is applied to the wire, heat is generated and transferred to the water, which in turn alters the refractive index. Along with an alteration in refractive index, the heating increases the buoyancy of water in contact with the wire,

2011 JINST 6 P03003

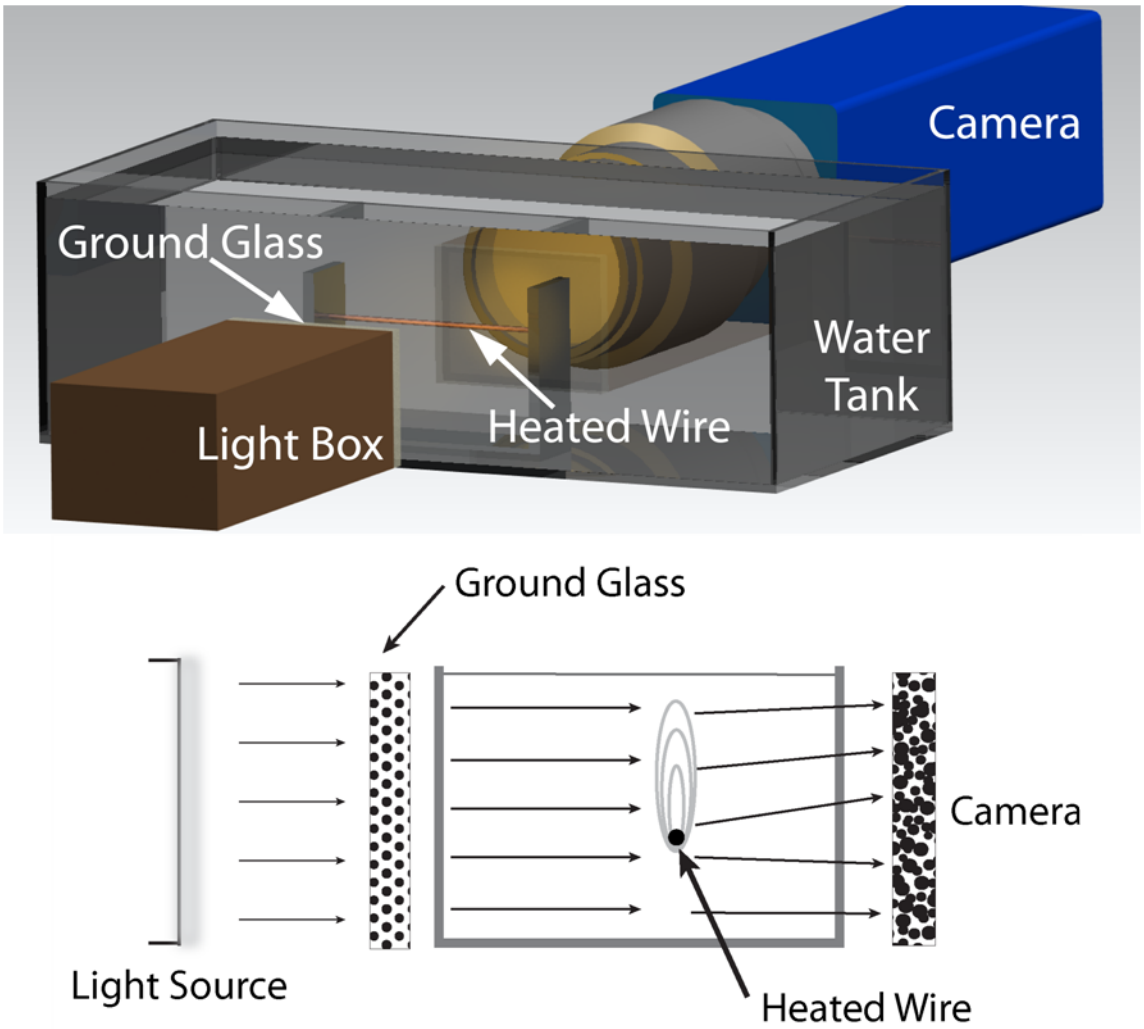

Figure 1. (Top) Schematic diagram of the experimental configuration used in this study. The camera and lens are focused on the textured surface on the front of the light box. In this case the surface was finely sand-blasted glass. (Bottom) Light is refracted by temperature gradients near the heated wire (used as a model of water heated by X-ray illumination) causing apparent motion of the textured surface when compared to images taken in a thermally homogenous state. The apparent motion is then measured using PIV analysis software and then integrated to an indicative temperature using RIT analysis software.

which over time begins to rise in a plume from the wire. The RIT system was used to record a sequence of images that after analysis, provides the changing refraction of ray paths, and from this the temperature can easily be calculated.

The recorded sets of images are discretized into sub-regions that correspond to sub-regions of the reference image and a PIV-type cross-correlation analysis is performed between these [35, 36]. The result of this analysis is a high-resolution map of the deflection of the light rays for the entire imaging region. This deflection is due the change in refractive index caused by heating from the wire.

2011 JINST 6 P03003

We used a one dimensional difference equation method to simulate thermal diffusion;

$$u_J^{N+1} = s\left(u_J^{N+1} - u_{J-1}^N\right) + (1-2s)u_J^N + u_J^0 \tag{2.1}$$

where $s = k\Delta t/(\Delta x)^2$. The times are 0, Δt, $2\Delta t$, ..., $N\Delta t$, and the positions are a, $a+\Delta x$, ..., $a+J\Delta x = b$, and $u(a+j\Delta t, n\Delta t)$ is the temperature at a given position and time. Δx is 2.5 μm and Δt is 0.2 μs. The microbeams are about 20 microns wide, 200 microns across and 12,000 microns long. The variation of dose with depth is of the order of 10% per 1000 microns. The heat diffusion problem is effectively one dimensional;

$$\frac{\partial u}{\partial t} = k\frac{\partial^2 u}{\partial x^2} \tag{2.2}$$

For water, $k = K/cp$, where K is the thermal conductivity of water, 0.58 W/m°K, C is the heat capacity of water, 4,181.3 J/kgK and ρ is the density of water, 997.0479 kgm^{-3}, $k = 1.4\,\mathrm{E}-07$ m^{2}s^{-1}, or 0.1439 μm$^2\mu$s^{-1}.

3 Results

Figure 2 shows a time series of the calculated temperature field on the plane over the heated wire serving as a model for the X-ray beam through a calorimeter. The wire extends horizontally along the bottom of each frame. The growing and then rising heat-plume is clearly resolved in both space and time and behaves exactly as can be expected. In (1), taken shortly after the wire heating is initiated, heating of the surrounding fluid is detectable along the bottom of the frame. In (2), an initially compact "mushroom-cap" plume of buoyant water has risen through approximately one quarter of the image plane, which can be identified by the strong horizontal band of yellow in the image. In (3) and (4), the head of the plume broadens vertically as it continues to convect upwards from the wire. Throughout these images, the heated wire remains visible. Note the total temperature change here is 12 degrees, 500 times greater than the expected temperature change from a 1 ms exposure on the Australian Synchrotron imaging and medical beamline, assuming an air kerma rate of 100 kGy/s and specific heat capacity C_p = 4180 Gy/degree K. At 1.0 ms, thermal diffusion will be the major cause of uncertainty in determining the peak to valley ratio, and we calculate thermal diffusion will reduce the measured peak to valley ratio to 76% of its initial value, but the individual microbeams will still resolve (figure 3).

4 Discussion

We describe in this article two potential methods of optical dosimetry for synchrotron MRT; Holographic Interferometry and Reference Image Topography with modified Particle Image Velocimetry. We present preliminary RIT/PIV data which demonstrates a clear proof-of-concept for the novel approach of utilizing a modified RIT method to measure X-ray dose delivered to a dosimeter. One may also resolve the variation of dose with depth by aligning, the measurement system with one of the two measurement axes along the z-axis. As a 2D imaging method, any two dimensions of the MRT dose distribution can be measured. In-fact all 3 axes could be resolved with 2 systems (e.g. one aligned on the xz plane and one on either the xy or yz planes).

2011 JINST 6 P03003

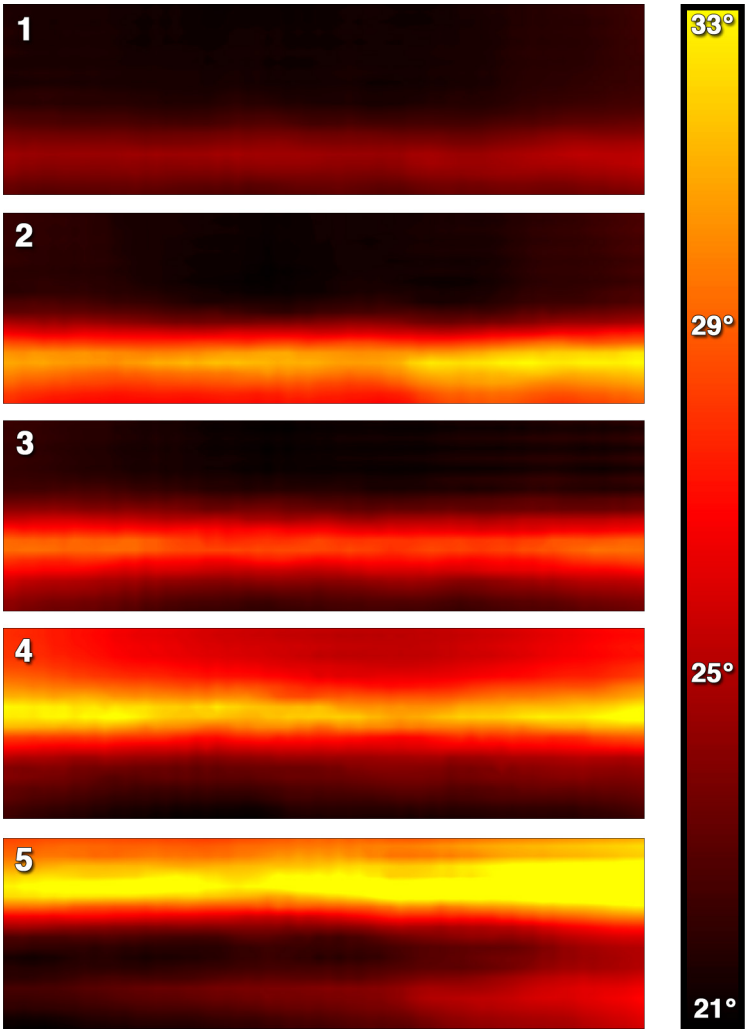

Figure 2. Contours of temperature measured using the modified RIT technique. The hot, horizontal band appearing at progressively higher positions above the wire in each frame is the head of a buoyant plume rising from the heated wire in water. The wire is located at the bottom of each frame, and is viewed from the side. Contour levels from black through to yellow show temperatures of 21 to 33 degrees Celsius respectively.

The use of a difference equation method allows us to easily model the steady deposit of heat during the exposure (represented by the constant u_J^0 term). The method is approximate but sufficient for the purpose, since the shape of the microbeam profile depends on the accuracy of the manufacture of the microbeam collimator, as well as basic x-ray physics. Although we have used a realistic approximation to the profile shapes from experimental data obtained from the medical beamline, the shape of the profile will strongly influence the rate of diffusion, and must ultimately be determined by experimental measurement. The difference equation method is therefore adequate and appropriate.

The broad synchrotron beam, is 2000 microns wide, and the effect of thermal diffusion is negligible. Hussmann [6] showed experimentally that for similar spatial resolution (5,300 micron diameter electron beam), significant change in the heat distribution was only observed after 300–

2011 JINST 6 P03003

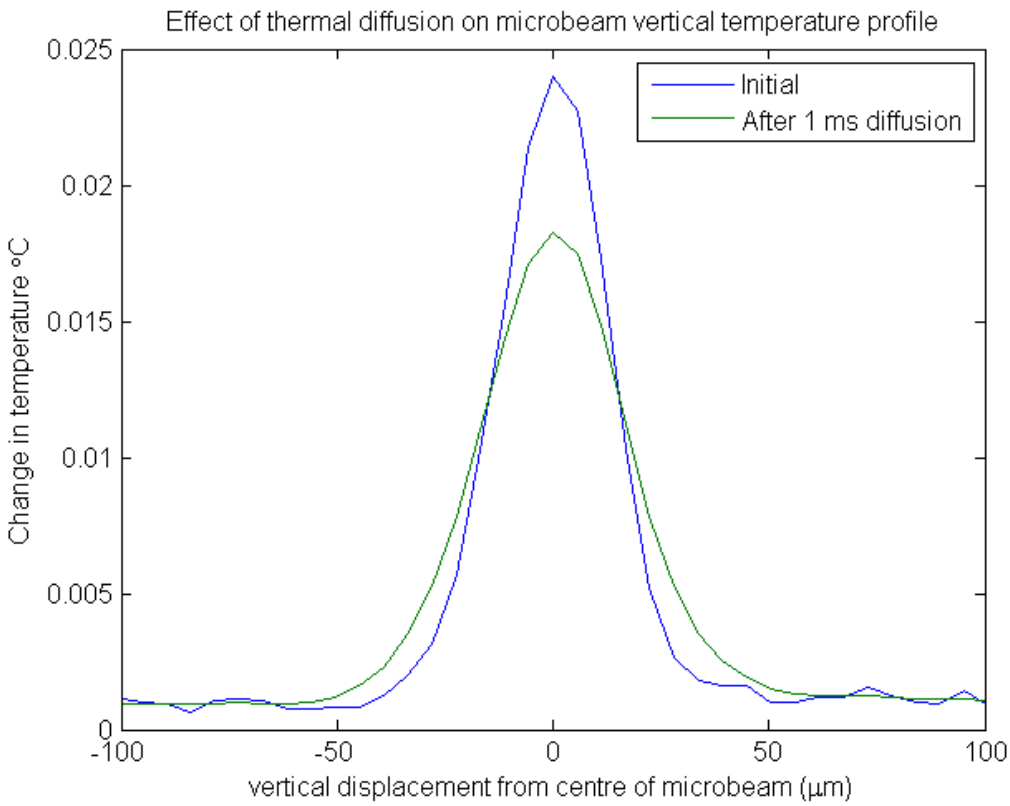

Figure 3. Vertical profile of temperature change from synchrotron microbeams, showing effect of 1 ms of heat diffusion in water. The initial profile is taken from microdensitometry scans of radiochromic films, scaled to meet the expected temperature change from a 1ms exposure on the Australian Synchrotron medical beamline.

400 msec [30]. At exposure times of this length, the temperature change is of the order of 6 degrees, comparable with the 12 degrees we used experimentally. Some of the energy deposited by the radiation is used up in chemical reactions, but this is estimated at 1% [6]. So for the broad synchrotron beam, 2% accuracy is conceivable, and would be an important achievement on its own. For the synchrotron microbeam, thermal diffusion becomes the limiting factor for two reasons;

1. It takes a finite time for the synchrotron beam to produce a change in refractive index sufficient to be detected.

2. It takes a finite time for the measurement of the heat distribution to be made, during which time the heat distribution is changing due to thermal diffusion.

It is important to re-iterate that PIV offers a very short measurement time; on the order of a microsecond, so the limiting factor is the synchrotron X-ray dose rate. The very short image acquisition time means that we may obtain 'sharp' or 'crisp' data which would be suitable for deconvolving the thermal effect because there is effectively no diffusion during the measurement.

For an exposure time of 1 msec, heat diffusion will reduce the peak to valley ratio to 76% of its actual value. Whilst it may be difficult to recover 2% accuracy from modeling the thermal diffusion,

2011 JINST 6 P03003

we should consider some of the available estimates of the measured peak-to-valley ratio currently have uncertainties of approximately ±25% (Crosbie et al. 2008). Additionally, the mechanism of heat diffusion is well understood, and easily modeled. By increasing the exposure time above 1 msec, we can create heat distributions that can be used to test our ability to back project to the heat distribution at 1 msec. In this way the projection back to 0 msec, and thus the dose distribution, can be verified experimentally.

Our aim is to have an optical calorimeter capable of measuring the absolute dose distribution for synchrotron-generated X-ray microbeams. If successful, it will have a major effect on the field of MRT and radiation metrology. Other MRT research groups around the world can be expected to adopt the optical calorimetry method of dosimetry for MRT. Importantly, we expect our proposed dosimeter to facilitate the introduction of MRT as a clinical treatment option for certain human cancers. Every radiotherapy technique needs a reliable method of measuring the absorbed dose in order for it to gain acceptance by the wider radiation oncology community. It is not sufficient to rely on Monte Carlo computer simulations of radiation transport. Our proposed method aims to resolve the question of MRT dosimetry and allow us to unequivocally characterise the absorbed dose distribution.

Synchrotron MRT has the potential to revolutionise the way radiotherapy is performed. Several groups [2, 3, 14, 15] including our own [1] have demonstrated effective tumour response with minimal side effects on tumours sites that are resistant to conventional radiotherapy. Such results demand that the underlying biological mechanisms of MRT be determined but this has been greatly impeded by the difficulty of accurately measuring the absorbed dose distribution. There is currently no single dosimeter with the dynamic range and spatial resolution to adequately measure the 2-dimensional MRT dose distribution, let alone the 3-dimensional distribution. An accurate, measurement-based system of dosimetry will undoubtedly contribute to the MRT knowledge base, and importantly, is essential if MRT is ever to be clinically accepted.

An optical calorimetry approach has the advantage that it does not impede or perturb the radiation beam and intrinsically provides the required resolution. Thermal diffusion of water after a 1.0 ms exposure is a major source of uncertainty with the optical calorimetry method. The challenge will be to extrapolate from different exposure times and deconvolve using the known thermal diffusion properties of water to achieve an accuracy of better than 10%.

Acknowledgments

We are grateful to the Faculty of Science, Monash University for providing seed funds which enabled us to obtain our preliminary results.

References

[1] J.C. Crosbie et al., *Tumor cell response to synchrotron microbeam radiation therapy differs markedly from cells in normal tissues*, *Int. J. Radiat. Oncol. Biol. Phys.* **77** (2010) 886.

[2] F.A. Dilmanian et al., *Response of rat intracranial 9L gliosarcoma to microbeam radiation therapy*, *Neuro-oncol.* **4** (2002) 26.

2011 JINST 6 P03003

[3] R. Serduc et al., *Synchrotron microbeam radiation therapy for rat brain tumor palliation-influence of the microbeam width at constant valley dose*, *Phys. Med. Biol.* **54** (2009) 6711.

[4] R. Serduc et al., *Brain tumor vessel response to synchrotron microbeam radiation therapy: a short-term in vivo study*, *Phys. Med. Biol.* **53** (2008) 3609.

[5] J.C. Crosbie et al., *A method of dosimetry for synchrotron microbeam radiation therapy using radiochromic films of different sensitivity*, *Phys. Med. Biol.* **53** (2008) 6861.

[6] E.K. Hussmann, *A holographic interferometer for measuring radiation energy deposition profiles in transparent liquids*, *Appl. Opt.* **10** (1971) 182.

[7] E.K. Hussmann and W.L. McLaughlin, *Dose-distribution measurement of high-intensity pulsed radiation by means of holographic interferometry*, *Radiat. Res.* **47** (1971) 1.

[8] *Imaging and measuring electron beam dose distributions using holographic interferometry*, *Nucl. Instrum. Meth.* **128** (1975) 337.

[9] E. Brauer-Krisch et al., *Effects of pulsed, spatially fractionated, microscopic synchrotron X-ray beams on normal and tumoral brain tissue*, *Mutat. Res.* **704** (2010) 160.

[10] A. Bravin, *The biomedical programs at the ID17 beamline of the European Synchrotron Radiation Facility*, Springer, (2007).

[11] R. Serduc et al., *In vivo two-photon microscopy study of short-term effects of microbeam irradiation on normal mouse brain microvasculature*, *Int. J. Radiat. Oncol. Biol. Phys.* **64** (2006) 1519.

[12] N. Zhong, G.M. Morris, T. Bacarian, E.M. Rosen and F.A. Dilmanian, *Response of rat skin to high-dose unidirectional x-ray microbeams: a histological study*, *Radiat. Res.* **160** (2003) 133.

[13] F.A. Dilmanian et al., *Murine EMT-6 carcinoma: high therapeutic efficacy of microbeam radiation therapy*, *Radiat. Res.* **159** (2003) 632.

[14] J.A. Laissue et al., *Neuropathology of ablation of rat gliosarcomas and contiguous brain tissues using a microplanar beam of synchrotron-wiggler-generated X rays*, *Int. J. Cancer* **78** (1998) 654.

[15] M. Miura et al., *Radiosurgical palliation of aggressive murine SCCVII squamous cell carcinomas using synchrotron-generated X-ray microbeams*, *Br. J. Radiol.* **79** (2006) 71.

[16] H.M. Smilowitz et al., *Synergy of gene-mediated immunoprophylaxis and microbeam radiation therapy for advanced intracerebral rat 9L gliosarcomas*, *J. Neurooncol.* **78** (2006) 135.

[17] J.A. Laissue et al., *The weaning piglet cerebellum: a surrogate for tolerance to MRT (microbeam radiation therapy) in paediatric neuro-oncology*, *Proc. SPIE* (Penetrating radiation systems & applications III) **4508** (2001).

[18] F.Z. Company and B.J. Allen, *Calculation of microplanar beam dose profiles in a tissue/lung/tissue phantom*, *Phys. Med. Biol.* **43** (1998) 2491.

[19] M. De Felici et al., *Dose distribution from x-ray microbeam arrays applied to radiation therapy: an EGS4 Monte Carlo study*, *Med. Phys.* **32** (2005) 2455.

[20] I. Orion et al., *Monte Carlo simulation of dose distributions from a synchrotron-produced microplanar beam array using the EGS4 code system*, *Phys. Med. Biol.* **45** (2000) 2497.

[21] E.A. Siegbahn, J. Stepanek, E. Brauer-Krisch and A. Bravin, *Determination of dosimetrical quantities used in microbeam radiation therapy (MRT) with Monte Carlo simulations*, *Med. Phys.* **33** (2006) 3248.

[22] G.I. Kaplan et al., *Improved spatial resolution by MOSFET dosimetry of an x-ray microbeam*, *Med. Phys.* **27** (2000) 239.

2011 JINST 6 P03003

[23] A. Rosenfeld et al., *MOSFET dosimetry of an X-ray microbeam*, *IEEE Trans. Nucl. Sci.* **46** (1999) 1774.

[24] E.A. Siegbahn et al., *MOSFET dosimetry with high spatial resolution in intense synchrotron-generated x-ray microbeams*, *Med. Phys.* **36** (2009) 1128.

[25] E. Brauer-Krisch et al., *MOSFET dosimetry for microbeam radiation therapy at the European Synchrotron Radiation Facility*, *Med. Phys.* **30** (2003) 583.

[26] M. Ptaszkiewicz, E. Brauer-Krisch, M. Klosowski, L. Czopyk and P. Olko, *TLD dosimetry for microbeam radiation therapy at the European Synchrotron Radiation Facility*, *Radiat. Meas.* **43** (2008) 990.

[27] A. Miller and W.L. McLaughlin, *Depth dose measurements using holographic interferometry*, *Radiat. Res.* **59** (1974) 225.

[28] W.L. McLaughlin, M.L. Walker and J.C. Humphreys, *Calorimeters for calibration of high-dose dosimeters in high-energy electron beams*, *Radiat. Phys. Chem.* **46** (1995) 1235.

[29] L.W. Tilton and J.K. Taylor, *Refractive index and dispersion of distilled water for visible radiation, at temperatures 0 to 60°C*, *J. Res. Nat. Bur. Stand.* **20** (1938) 419.

[30] A. Miller and W.L. McLaughlin, *Imaging and measuring electron beam dose distributions using holographic interferometry*, *Nucl. Instrum. Meth.***128** (1975) 337.

[31] G. Abbate, U. Bernini, E. Ragozzino and F. Somma, *The temperature dependence of the refractive index of water*, *J. Phys.* **D 11** (1978) 1167.

[32] F. Charriere et al., *Cell refractive index tomography by digital holographic microscopy*, *Opt. Lett.* **31** (2006) 178.

[33] J. Sheng, E. Malkiel and J. Katz, *Digital holographic microscope for measuring three-dimensional particle distributions and motions*, *Appl. Opt.* **45** (2006) 3893.

[34] R. Hooke, *Of a new property in the air*, *Micrographia* Observation LVIII (1665) 217.

[35] A. Fouras, K. Hourigan, M. Kawahashi and H. Hirahara, *An improved, free surface, topographic technique*, *J. Visualization* **9** (2006) 49.

[36] A. Fouras, D. Lo Jacono, G.J. Sheard and K. Hourigan, *Measurement of instantaneous velocity and surface topography in the wake of a cylinder at low Reynolds number*, *J. Fluid Struct.* **24** (2008) 1271.

[37] R.J. Adrian, *Twenty years of particle image velocimetry*, *Exp. Fluids* **39** (2002) 159.

[38] A. Fouras, D. Lo Jacono and K. Hourigan, *Target-free stereo PIV: A novel technique with inherent error estimation and improved accuracy*, *Exp. Fluids* **44** (2008) 317.

2011 JINST 6 P03003